



HAL
open science

Modeling isogenic cancer cell response upon varying TRAIL stimulations to decipher the kinetic determinants of cell fate decision

Marielle Péré, Diego A. Oyarzun, Jérémie Roux, Madalena Chaves

► To cite this version:

Marielle Péré, Diego A. Oyarzun, Jérémie Roux, Madalena Chaves. Modeling isogenic cancer cell response upon varying TRAIL stimulations to decipher the kinetic determinants of cell fate decision. Foundations of Systems Biology in Engineering (FOSBE), Aug 2022, Cambridge, Massachusetts, United States. hal-03868311

HAL Id: hal-03868311

<https://hal.science/hal-03868311v1>

Submitted on 23 Nov 2022

HAL is a multi-disciplinary open access archive for the deposit and dissemination of scientific research documents, whether they are published or not. The documents may come from teaching and research institutions in France or abroad, or from public or private research centers.

L'archive ouverte pluridisciplinaire **HAL**, est destinée au dépôt et à la diffusion de documents scientifiques de niveau recherche, publiés ou non, émanant des établissements d'enseignement et de recherche français ou étrangers, des laboratoires publics ou privés.

Modeling isogenic cancer cell response upon varying TRAIL stimulations to decipher the kinetic determinants of cell fate decision

Marielle Péré^{*,**,**} Diego Oyarzun^{*} Jérémie Roux^{**,**}
Madalena Chaves^{**}

^{*} *School of Informatics, University of Edinburgh, Edinburgh EH8 9AB, United Kingdom (e-mail: marielle.pere@inria.fr)*

^{**} *Université Côte d'Azur, Inria, INRAE, CNRS, Sorbonne Université, Biocore team, Sophia Antipolis, France*

^{***} *Université Côte d'Azur, CNRS UMR 7284, Inserm U 1081, Institut de Recherche sur le Cancer et le Vieillissement de Nice, Centre Antoine Lacassagne, 06107 Nice, France*

Abstract: Cell response heterogeneity upon drug treatment is a leading cause of reduced drug efficacy in preclinical cancer research. Although single-cell studies have revealed the depth of cellular heterogeneity observed between in tumor cells, the regulatory impact of cell variability on therapeutic response remains unclear.

Here, we present a new ODE model of the extrinsic apoptosis initiation by death-ligands. This model is calibrated on fluorescent time-trajectories (FRET) of hundreds of clonal HeLa cells treated with different amounts of Tumor necrosis factor-related apoptosis-inducing ligand (TRAIL). By highlighting the different steps in the regulation of apoptosis, and the associated timeline, we locate an initial cell fate decision just after TRAIL binding and the presence of additional regulation at the receptor that only benefits the drug-sensitive population. Then, our study provides evidence that increasing the dose of TRAIL actually has small effects within each population (resistant or sensitive) but rather accentuates the differences between the two, affecting the population dynamics in two different ways depending on their response to the drug. Finally, the distribution of 3 parameters of our mechanistic model, according to the cell drug response, suggests the existence of a determinant threshold in C8 dynamics, independent of the drug dose, that distinguishes cells drug-resistant or sensitive, that could be used to control or predict cell drug-response in the future.

Keywords: Apoptosis, Pharmaco-kinetics, Fractional killing, Oncology, Single-cell, ODE.

1. INTRODUCTION

Fractional killing due to non-genetic resistance is a major cause of therapeutic failure in preclinical assays of anticancer drugs, and the actual manifestation of drug efficacy. Indeed, all isogenic cells - sometimes in the same phenomenological state (Purvis et al., 2012) - respond to cytotoxic drugs with different timing and magnitude, but only a fraction of them commit to apoptosis, a form of programmed cell death (Roux et al., 2015). Additionally, repeated experiments on several generations of clonal resistant cells (Flusberg et al., 2013), have shown that the same amount of sensitive cell is always observed in each round, even with saturating doses. Combined, this heterogeneous commitment to apoptosis on several generations leads to drug evasion, incomplete tumor clone eradication, and at the end, treatment failure (Strasser and Vaux, 2020).

Several studies combining mathematical modelling - (Albeck et al., 2008; Matveeva et al., 2019) - and single-cell omics data - gene level:(Purvis et al., 2012), signal

transduction (Roux et al., 2015), multi-omic scale (Paek et al., 2016) - have established several potential sources for this partial response to cancer drugs in isogenic populations at all omics stages, some of them directly linked to cell signalling dynamics and other coming from stochastic noise (Hurbain et al., 2020). However, none of these studies were interested in the timeline of cell decision despite the increasing number of articles revealing the key-role of chemical reaction speed and timing in cell decision (Paek et al., 2016; Roux et al., 2015). Indeed, we believe that the moment a cell takes its lethal decision tells us a long story about its sensitivity state (Meyer et al., 2020) and how we could predict and control its drug response.

In this study, we present an ODE model of extrinsic apoptosis triggered by death receptor ligands, calibrated on single-cell fluorescent ratio time-trajectories (FRET - Albeck et al. (2008)), of clonal HeLa cells, from Roux et al. (2015). These cells are treated with 4 different doses of Tumor necrosis factor-related apoptosis-inducing ligand (TRAIL), a death-ligand drug known for its high rate

of resistant cells in clonal populations (fractional killing), even at saturating dose, and change in fluorescence when they react to the drug.

Analysing the timeline of the core reactions and the dynamic properties of the model with a principal process analysis, we identify regulatory steps of the cell decision, locating a first resolution upon TRAIL binding but also the existence of a ruling time frame during which the sensitive cells benefit from additional regulation at the receptor level, before cell death commitment. Comparing the mean timeline of the death inducing signalling complex (DISC) formation, according to the drug response when TRAIL dose increases, we show that this augmentation has different impacts, whether the cell is sensitive to the drug, or resistant. In particular, this study reveals that an increase in TRAIL doesn't affect so much the cell parameters and timeline inside each population (resistant and sensitive) but rather widens the gap between the resistant and sensitive cells. Finally, the distribution of three parameters of an approximated solution of our model - parameters directly related to caspase 8 activity - shows the existence of a clear biological threshold distinguishing sensitive from resistant cells, regardless of the drug dose. The double partitioning of these parameters highlights the central role of caspase 8 and paves the way for the prediction and control of the cellular response to drugs at the single cell level.

2. MODELING TRAIL-INDUCING EXTRINSIC APOPTOSIS

Mechanistic models of extrinsic apoptosis (Albeck et al., 2008; Chaves et al., 2021) usually consider many chemical reactions and proteins, sometimes too many to understand the role of each compound. Following this idea, in a previous work, we determined the key-proteins of extrinsic apoptosis transcriptional pathway (Péré et al., 2020). Therefore, our current Extrinsic Apoptosis Initiation Core Reactions model (EAICRm), obtained by applying mass action kinetic law (Fig. 1), only integrates the receptor (R) trimerisation when TRAIL (T) binds to the cell, while it does not represent FADD and c-FLIP actions.

The major novelty of this system is incorporating all the steps leading to $C8$ activation, whether with the dimerisation of $pC8$ (p for pro, C for caspase), or with the recruitment of an already active $C8$. Hence, the dimerisation of $pC8$, which is required to activate $C8$, is modelled, as well as the $C8/C10$ clustering and the downstream feedback loop on $C8$. As in (Péré et al., 2020), the effector caspases are grouped under the variable C^{eff} , and the intermediary complexes are denoted by Zi , $i \in \{0, 1, 2\}$. Finally, the model also accounts for the FRET activation by $C8$.

3. PRINCIPAL PROCESS ANALYSIS (PPA)

A PPA (Casagrande et al., 2018) evaluates the impact of each chemical reaction (represented by each equation term) on each protein (variable) all along the system simulation.

The EAICR parameters were estimated for each cell of the dataset from Roux et al. (2015). This study records FRET time trajectories of clonal HeLa cells treated with

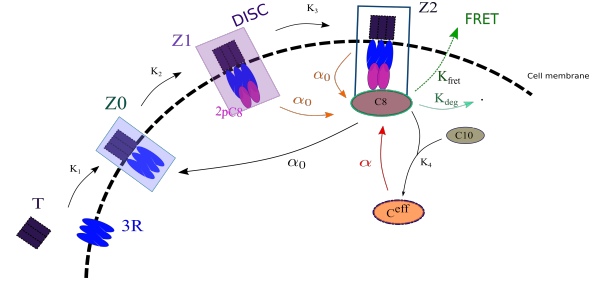


Fig. 1. **Extrinsic Apoptosis Initiation Core Reactions model (EAICRm) scheme**

50ng/mL of TRAIL ($T_0 = 1550$ molecules), and observed for 10 hours. The calibration method is from Péré et al. (2020). Then, each fitted system were analysed with the PPA method.

3.1 Describing apoptosis dynamic timeline

To run a PPA, we first must split the simulation into **characteristic time checkpoints**. We decided to base their definition on dynamic events (rather than using same-size steps) and divide our 10 hours of simulations into important time-slots corresponding to specific protein dynamic turnovers (in italic the mean value in min for cells treated with 50ng/ml of TRAIL (app. C for computation):

- (1) $\tau_{T.trigger}$ ($1e-5$): $Z0$ reaches its first local maximum - it corresponds to the moment when TRAIL is in sufficient quantity to trigger a cellular reaction;
- (2) $\tau_{DISC.ass}$ (1.15): at this time, the DISC assembly expands, R decreasing speed strongly draws down and $pC8$ becomes linear;
- (3) $\tau_{drug.0}$ (5.20): T falls down to the equilibrium $T = 0$, R stabilizes to $-3T_0 + R_0$ while $Z1$ reaches its local maximum $Z1 = T_0$;
- (4) $\tau_{DISC.end}$ (400): $Z1$ collapses to almost 0 and $Z0$ becomes bigger than $pC8$;
- (5) $\tau_{C8.final}$ (412): $C8$ reaches its maximum before decreasing (or remaining constant for the major part of sensitive cells)

Hence, we obtain 6 models summarised in table 1 p.3.

3.2 An early cell decision time

The PPA shows that the first changes between sensitive and resistant population happen after $\tau_{T.trigger}$ and continue until cell death (before $\tau_{DISC.end}$ for the sensitive), which locates the main events leading to fractional killing between these two times. Comparing resistant and sensitive dynamic during this timelapse reveals that $\overline{K_2}Z1$ comes into action sooner in the sensitive population and potentially add a regulatory effect on the DISC in the form of a positive feedback, driving the cell to death.

Table 1 also highlights the significant impact of $Z0$ (T:R) and $Z1$ (DISC - T:R:2pC8) on every step of the cell fate. These complexes appear to be the decision-makers whereas $C8$ is simply the result of their actions.

Finally, $\tau_{drug.0}$ marks the moment when the effective caspase downstream feedback is activated but, at least in this model, they seem not to have enough impact to really influence the cell's decision in most cases. We can also

Table 1. Principal Process Analysis Results - Only the reactions above 0.05 (in black) and the one above 0.0005 (in blue) for more than half of the cells (more than 57 cells for resistant and 150 for the sensitive population) are kept. The reactions available only for the sensitive population, and between 0.0005 and 0.05, are in purple and the sensitive reaction above 0.05 in red.

var.	All experience	[0 $\tau_{T.trigger}$]	$]\tau_{T.trigger}, \tau_{DISC.ass}]$	$]\tau_{DISC.ass}, \tau_{drug.0}]$	$]\tau_{drug.0}, \tau_{DISC.end}]$	$]\tau_{DISC.end}, \tau_{C8.final}]$	$]\tau_{C8.final}, \tau_{cell.death}]$
\dot{T}	$-K_1 TR^3$				$+\overline{K_1} Z0$	$+\overline{K_1} Z0$	$+\overline{K_1} Z0$
\dot{R}	$-3K_1 TR^3$				$+3\overline{K_1} Z0$	$+3\overline{K_1} Z0$	$+3\overline{K_1} Z0$
$\dot{Z}0$		$K_1 TR^3$ $-K_2 Z0pC8^2$	$K_1 TR^3 + \alpha_0 Z1$ $-K_2 Z0pC8^2$ $+\overline{K_2} Z1$	$K_1 TR^3 + \alpha_0 Z1$ $-K_2 Z0pC8^2$ $+\overline{K_2} Z1$	$+K_1 TR^3 + \alpha_0 Z1$ $-K_2 Z0pC8^2$ $+\overline{K_2} Z1$	$K_1 TR^3 + \alpha_0 Z1$ $-K_2 Z0pC8^2 - \overline{K_1} Z0$ $+\overline{K_2} Z1$	$K_1 TR^3 + \alpha_0 Z1$ $-K_2 Z0pC8^2$ $-\overline{K_1} Z0$ $-\overline{K_1} Z0$ $+\overline{K_2} Z1$
$p\dot{C}8$	$-K_2 Z0pC8^2$			$2\overline{K_2} Z1$	$+2\overline{K_2} Z1$	$+2\overline{K_2} Z1$	$+2\overline{K_2} Z1$
$\dot{Z}1$	$K_2 Z0pC8^2$		$-\alpha_0 Z1 - \overline{K_2} Z1$	$-\alpha_0 Z1 - \overline{K_2} Z1$	$-\alpha_0 Z1 - \overline{K_2} Z1$	$-\alpha_0 Z1 - \overline{K_2} Z1$	$-\alpha_0 Z1 - \overline{K_2} Z1$
$\dot{Z}2$	$K_3 Z1C8$			$-\overline{K_3} Z2 - \alpha_0 Z2$	$-\overline{K_3} Z2 - \alpha_0 Z2$	$-\overline{K_3} Z2 - \alpha_0 Z2$	
C^{eff}	$K_4 C10Z2$				$-\alpha C^{eff}$	$-\alpha C^{eff}$	$-\alpha C^{eff}$
$\dot{C}10$	$-K_4 C10Z2$				αC^{eff}	αC^{eff}	αC^{eff}
$\dot{C}8$	$\alpha_0 Z1$	$-K_{deg}C8$			$-K_{deg}C8$	$-K_{deg}C8$	$-K_{deg}C8$
\dot{FRET}	$K_{fret}C8$						

notice that C8 degradation disappears just after TRAIL binding, during the DISC formation phase. However, after $\tau_{drug.0}$, it keeps gaining importance until $\tau_{C8.final}$. In summary, it seems clear that cells take a first decision before $\tau_{drug.0}$. But the mechanisms responsible for cell fate implementation and regulation are really acting between $\tau_{DISC.ass}$ and $\tau_{DISC.end}$.

3.3 Reducing Extrinsic Apoptosis Initiation Core Reaction model

The PPA method is originally designed to reduce the model size. Removing the chemical reactions important only for themselves all along the experiment, we obtain a reduced EAICR model (**rEAICR**):

$$\begin{cases} \dot{T} = -K_1 TR^3 + \overline{K_1} Z0, \\ \dot{R} = -3K_1 TR^3 + 3\overline{K_1} Z0, \\ \dot{Z}0 = K_1 TR^3 - \overline{K_1} Z0 + K_2 Z0pC8^2 \\ \quad + \overline{K_2} Z1 + \alpha_0 Z1, \\ p\dot{C}8 = -2K_2 Z0pC8^2 + 2\overline{K_2} Z1, \\ \dot{Z}1 = K_2 Z0pC8^2 - \overline{K_2} Z1 - \alpha_0 Z1, \\ \dot{C}8 = \alpha_0 Z1 - (K_{deg} + K_{fret})C8, \\ \dot{FRET} = K_{fret}C8. \end{cases} \quad (1)$$

Using mass conservation:

$$\dot{T} + \dot{Z}1 + \dot{Z}0 = 0. \quad (2)$$

As Z0 and Z1 are intermediary complexes, they are null at the beginning of the experiment and we get the following relation:

$$T + Z1 + Z0 = T_0. \quad (3)$$

Model simulation (data not shown but simulation parameters available), with different cell sets of parameters, show that between $\tau_{drug.0}$ and $\tau_{DISC.end}$,

$$Z1 \approx T_0, \quad (4)$$

that leads to:

$$p\dot{C}8 = -2\alpha_0 T_0, \quad (5)$$

which gives us the slope of pC8 when it becomes linear. Hence, we approximate Z1 and Z0 with step functions by

putting $Z1 = T_0$ between 0 and $\tau_{DISC.end}$ (as $\tau_{drug.0}$ is 6 min), and assuming $Z1 = 0$ after $\tau_{DISC.end}$ in C8 and FRET). Therefore, before $\tau_{DISC.end}$,

$$\dot{C}8 = \alpha_0 T_0 - (K_{deg} + K_{fret})C8, \quad (6)$$

so an approximated explicit solution for C8 is given by :

$$C8_{0,\tau_{DISC.end}} = C8_0 e^{-t(K_{deg}+K_{fret})} + \frac{\alpha_0 T_0 (1 - e^{-t(K_{deg}+K_{fret})})}{(K_{deg} + K_{fret})}. \quad (7)$$

Integrating this solution in FRET equation:

$$FRET = \frac{K_{fret}}{K_{deg} + K_{fret}} \times \left(\alpha_0 T_0 t + \left(C8_0 - \frac{\alpha_0 T_0}{K_{deg} + K_{fret}} \right) (1 - e^{-(K_{deg}+K_{fret})t}) \right) \quad (8)$$

Setting:

$$\begin{cases} \beta_0 = K_{deg} + K_{fret}, \\ \beta_1 = \frac{K_{fret}\alpha_0 T_0}{\beta_0}, \\ \beta_2 = \frac{K_{fret}C8_0 - \beta_1}{\beta_0}, \end{cases} \quad (9)$$

we find a sigmoid formula for FRET :

$$FRET = (\beta_1 t + \beta_2 (1 - e^{-\beta_0 t})). \quad (10)$$

Keeping the same notation, between $\tau_{DISC.end}$ and $\tau_{C8.final}$:

$$\begin{cases} \dot{Z}1 = 0, \\ \dot{C}8 = -\beta_0 C8. \end{cases} \quad (11)$$

Hence,

$$\begin{cases} C8 = C8_{\tau_{DISC.end}} e^{-\beta_0(t-\tau_{DISC.end})}, \\ FRET = \frac{K_{fret}C8_{\tau_{DISC.end}}}{\beta_0} (1 - e^{-\beta_0(t-\tau_{DISC.end})}) + FRET(\tau_{DISC.end}). \end{cases} \quad (12)$$

Equations (10) and (12) provide an approximated explicit solution, denoted by **FRETexp**, for the time interval $[0, \tau_{DISC.end}]$, and between $\tau_{DISC.end}$ and the cell death, respectively.

From this analysis, we improved our fitting method for the next steps by using the FRETexp solution parameters to have a better initial guess (see B) and divide our fitting time by 4. It also gives a good idea of the main protagonists of the extrinsic apoptosis ($C8_0$, $pC8_0$, K_{deg} and α_0).

Lastly, taking the power series of this explicit solution recovers the empiric model from Roux et al. (2015), thus confirming the straightforward model suggested in that paper, as a simplification of a mechanistic and more detailed signaling pathway.

4. TRAIL VARIATION IMPACT

To understand how TRAIL dose variations affect cell decision, the rEAICR model parameters (and the corresponding characteristic times) were estimated for each cell of 4 datasets from Roux et al. (2015), treated with 4 different doses of TRAIL (5,10,25 and 50 ng/mL), using our new fitting method (see B), and imposing the same T_0 for all the cells treated with the same amount of TRAIL (see A).

4.1 Measuring TRAIL effects on timeline

To characterize TRAIL variation effects on the cell timeline, the 5 characteristic time checkpoints - $\tau_{T.trigger}$, $\tau_{DISC.ass}$, $\tau_{drug.0}$, $\tau_{DISC.end}$, $\tau_{C8.final}$ - are computed for all the cells, along with 4 associated time-lapses:

- (1) **DISC formation phase (DISC-fp - $[0, \tau_{drug.0}]$):** during this time-interval, Z_0 reaches a maximum before decreasing to 0. It seems that this time correspond to the reception of the apoptotic message sent by TRAIL binding on the cell. Then, when Z_0 reaches 0, the DISC complex starts to form : T decreases toward 0 (all cells go toward the same model equilibrium space $T = 0$), marking the end of signal reception, R decreases until $\tau_{DISC.ass}$ toward the value $-3T_0 + R_0$ (with mass conservation). $pC8$ lowers too.
- (2) **DISC action phase (DISC-ap - $]\tau_{DISC.ass}, \tau_{DISC.end}]$):** Z_1 represent the DISC in the system. From $\tau_{DISC.ass}$, and until $\tau_{DISC.end}$, Z_1 reaches its maximum level and remains constant so we consider this time-lapse as the DISC action. In addition, $\tau_{DISC.ass}$ marks a turn-over in $pC8$ dynamics as $pC8$ becomes linear. During this time, Z_0 starts to increase but very slowly, leading to the subsequent decrease of Z_1 , initiating the end of the phase and the major dynamic turn-over.
- (3) **C8 final decision (C8-fd - $]\tau_{DISC.end}, \tau_{C8.final}]$):** the DISC influence is finished, only $C8$ keeps evolving. The sensitive cells never reach this point but for the resistant population, we think this is the last chance to turn then into sensitive.
- (4) **C8 no possible turning back (C8-nptb - after $\tau_{C8.final}$ until death)**

Between $\tau_{DISC.ass}$ and $\tau_{drug.0}$, the two DISC involved phases **DISC-fp** and **DISC-ap** overlap.

4.2 TRAIL dose influences the early stages of apoptosis

Comparing the distribution of the characteristic times, and the associated time-lapses (only the mean value is represented in Fig. 2-(c-1)), shows that an increase in TRAIL affects mostly the beginning of apoptosis initiation (before $\tau_{drug.0}$) in two different ways according to the drug response.

For the resistant cells, more TRAIL means an earlier death

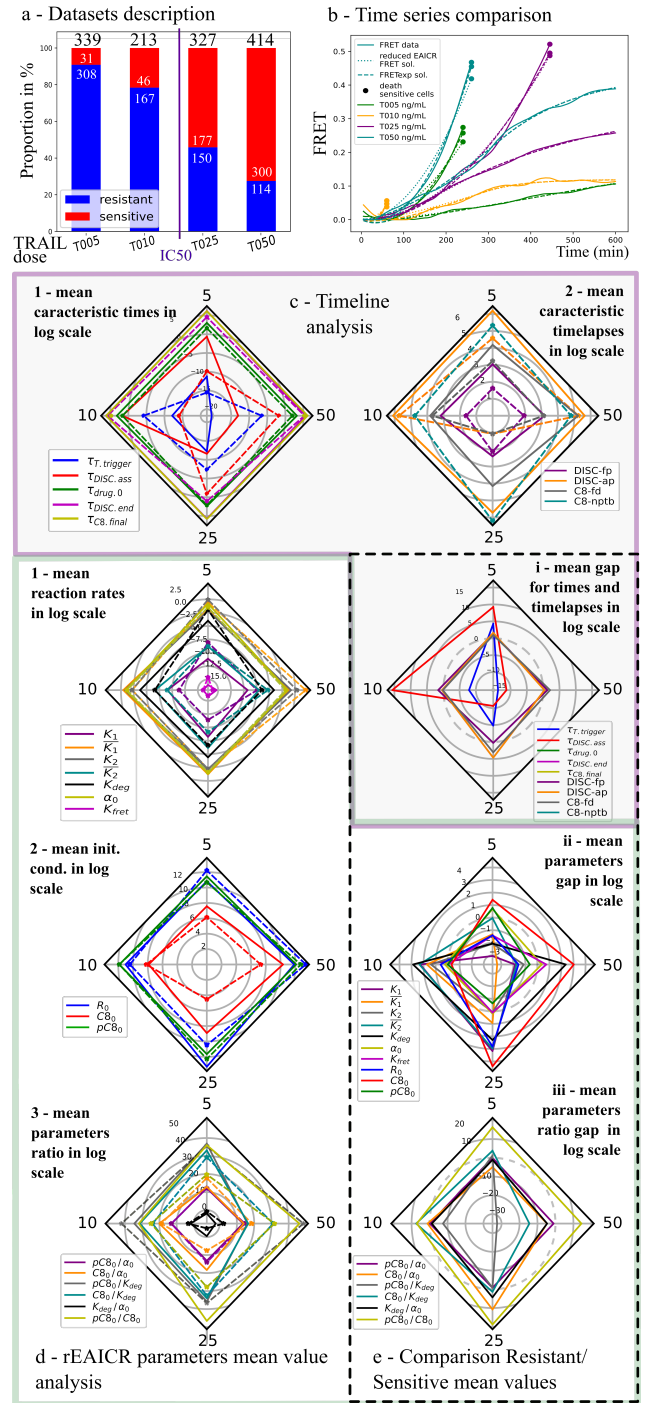


Fig. 2. Summary of the rEAICR model analysis for the 4 drug doses (timeline and parameter means distribution): a) Datasets description (Roux et al., 2015); b) Comparison of the time-series obtained with rEAICR model, the FRETexp solution and the real FRET measurements for a sensitive and a resistant cell of each dataset; c,d,e) Radar plots analysis according to the TRAIL dose in ng/mL (1 dose=1 vertex): c) Mean timeline analysis according to the drug response (sensitive in dashed line, resistant in plain); d) Mean rEAICR parameter (init. cond. and r. rates) values analysis according to the drug response; e) Comparison between resistant and sensitive mean values ($gap = \frac{mean R}{mean S}$)

signal trigger ($\tau_{T.trigger}$ is decreasing meaning that Z0 (T:R) reaches a first maximum earlier), smaller $\tau_{DISC.ass}$ and smaller DISC action phase too, but a longer C8-final decision phase. On the opposite side, the sensitive cells benefit from bigger $\tau_{T.trigger}$ and $\tau_{DISC.ass}$ with a bigger DISC formation phase too. However, the other time-lapses do not seem linked to the TRAIL dose since they are only notably changing at the IC50 (Fig. 2 -(c-2)).

Finally, the fraction between the mean time values for resistant and sensitive cells confirms that the main differences between them are located before $\tau_{drug,0}$ for all doses of drug, with strong variations for $\tau_{T.trigger}$ and $\tau_{DISC.ass}$ between the two populations, when TRAIL increases (Fig. 2-(e-i)). However, these variations does not affect the gap between resistant and sensitive in time-lapses. Indeed, for the time intervals, the biggest gaps, between resistant and sensitive cells, are observed for the DISC action phase and the C8-final decision interval, but at the IC50 (25 ng/mL), whereas it remains constant for the others TRAIL doses.

4.3 TRAIL variation differently impacts cells according to their drug sensitivity

Figure 2-d/e compares the mean value for each of the 7 reaction rates, the 3 initial conditions of the rEAICR model and the relative proportions (represented by a fraction) of the 4 main protagonists of the extrinsic apoptosis ($C8_0$, $pC8_0$, K_{deg} and α_0), as a function of drug response and TRAIL dose received. This comparison reveals that an increase in TRAIL has a more profound impact on the reaction rate of sensitive cells, particularly on the rates involved in the onset of the extrinsic apoptosis chain reaction. In particular, \bar{K}_1 , K_2 (associated to the Z0 complex in the model) increase while K_{deg} decreases for the sensitive cells (Fig. 2-(d-1)). Theses variations suggest that an increase in TRAIL lowers down C8 degradation for the sensitive population whereas it does not affect the C8 degradation rate for the resistant cells. Regarding the initial conditions (Fig. 2-(d-2)), the sensitive population also benefits from an increase in R_0 when the initial dose of TRAIL is higher.

For the resistant population, the augmentation of TRAIL mainly affects the quantity of recruited proteins. Indeed, the higher TRAIL is, the more R and $C8$ are initially recruited for the resistant population. On the other hand, the variation of TRAIL does not have such an impact on their reaction rates, as shown by the average values of the reaction rates as a function of the variation of TRAIL.

Comparing the evolution of $pC8_0$ upon TRAIL variation, for the two phenotypes (resistant and sensitive), highlights the fact that, even though the variation of $pC8_0$ is not so important within each population, the deviation between resistant and susceptible increases as TRAIL increases (Fig. 2-(e-ii)). These two distinct progressions according to the drug phenotypes are even more pronounced if we compare the relative proportions between initial conditions and reactions rates for $C8_0$, $pC8_0$, K_{deg} and α_0 (Fig. 2 (d-3) and (e-iii)).

Interestingly, for the parameters of the rEAICR model, the largest differences in initial conditions and in the reactions rates between resistant and sensitive, cells are obtained at the IC50 of TRAIL (25ng/mL) (Fig. 2 - e).

In conclusion, an increase in TRAIL does not have a great

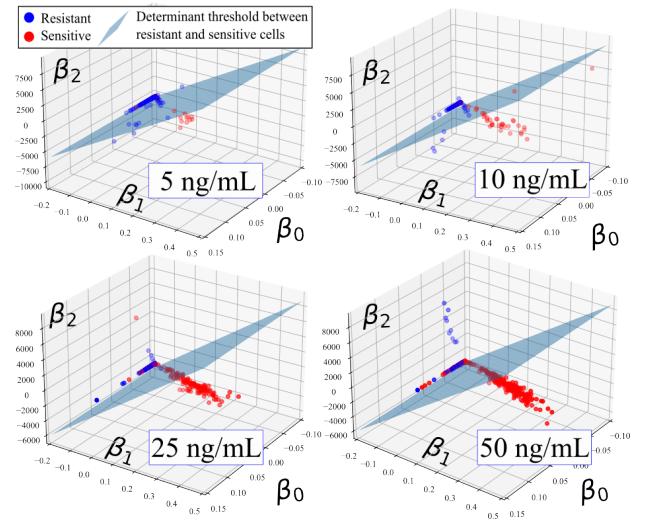


Fig. 3. **FRETexp β parameters distribution** according to the drug response and **common cell decision threshold** between life and death obtained with an linear support vector classifier (> 85% of accuracy)

impact on the reactions rates or the initial conditions within the two populations (resistant and sensitive) - even though it significantly extends the ratio between initial conditions and reactions rates. However, this drug augmentation considerably enlarges the differences between the two drug response populations, especially in the early stages of apoptosis initiation (before $\tau_{drug,0}$).

4.4 A clear distinction between survival and death

Fig.3 reveals two distinct distributions for the FRETexp parameters, whether cells are drug resistant or sensitive, regardless of the initial amount of TRAIL. As the FRETexp β depend on the initial amount of C8, but also on the degradation (K_{deg}) and the activation rate (α_0) of the initiator caspase (eq. 9), their dual distribution is a sign of a complex biological threshold, with predictive value, around C8 activity, that distinguishes cells in a sensitivity or resistant state, but also confirms the central role of C8 in apoptosis (Roux et al., 2015).

Indeed, Fig. 3 reveals the conditions (reaction rate and initial amount of protein) that cells must meet to be in a susceptible state, thus paving the way for controlling the cellular response to drugs. This clear difference between the two phenotypes also offers a possible way to predict cell drug response. Using only these 3 mechanistic parameters and our location of the cell death decision time, we may have the opportunity to create a new predictor of the apoptotic decision.

5. DISCUSSION

In this study, we presented a new ODE model of TRAIL-triggered extrinsic apoptosis initiation (EAICR) and used it to analyze the timeline of cell fate decision. By studying the dynamic balance between the proteins involved in extrinsic apoptosis initiation, and the associated timing for each cell, we **located an initial cell fate decision** just after TRAIL binding which leads to a **reduction of our model (rEAICR)** that recovers an **explicit expression**

for the caspase 8 and FRET early dynamics. The rEAICR model was next much more accurately fitted for all the isogenic cells in 4 datasets from the same study (Roux et al., 2015), varying TRAIL doses from 5 ng/mL to 50 ng/mL. The characteristic time distributions obtained from these data demonstrated that an **increase in TRAIL** has a more profound impact on the onset of cell commitment to apoptosis, but with **two different ways of changing the cell fate timeline depending on the sensitivity state of the cell**. The different ways in which resistant and sensitive cells evolve, when the dose of TRAIL varies, are caused by distinct model parameter distribution changes: sensitive cells are characterized by an increase in their reaction rates, while the resistant population is more affected in terms of the initial amount of protein. Overall, we show that **increasing TRAIL dose amplifies the gap between resistant and sensitive cells** as reflected in the values of the reaction rates, the amount of protein recruited, and especially the ratio between the initial amount of proteins and the reactions rates inside each of the two populations which shift in opposite ways according to the drug response phenotype. Finally, the parameter distribution of the approximated solution of the reduced EAICR model helps deciphering how C8 dynamic affects cell decision, but also suggests a **potential mean of predicting (and potentially controlling) drug response for any drug dose**.

ACKNOWLEDGEMENTS

All authors were supported by an INCa Plan Cancer Biologie Des Systèmes, ITMO Cancer (proposel IMoDRez, no.18CB001-00), and by Agence Nationale de la Recherche “Investissements d’Avenir” programs: LABEX SIGNALIFE ANR-11-LABX-0028-01 and IDEX UCAJedi ANR-15-IDEX-01. MP was supported in part by an Inria-Inserm PhD fellowship “Médecine Numérique” and by the RSE Saltire early career fellowship.

REFERENCES

- Albeck, J.G., Burke, J.M., Spencer, S.L., Lauffenburger, D.A., and Sorger, P.K. (2008). Modeling a snap-action, variable-delay switch controlling extrinsic cell death. *PLoS Biol*, 6(12), e299.
- Casagrande, S., Touzeau, S., Ropers, D., and Gouzé, J.L. (2018). Principal process analysis of biological models. *BMC systems biology*, 12(1), 1–26.
- Chaves, M., Gomes-Pereira, L.C., and Roux, J. (2021). Two-level modeling approach to identify the regulatory dynamics capturing drug response heterogeneity in single-cells. *Scientific reports*, 11(1), 1–15.
- Flusberg, D.A., Roux, J., Spencer, S.L., and Sorger, P.K. (2013). Cells surviving fractional killing by trail exhibit transient but sustainable resistance and inflammatory phenotypes. *Molecular biology of the cell*, 24(14), 2186–2200.
- Hurbain, J., Labavić, D., Thommen, Q., and Pfeuty, B. (2020). Theoretical study of the impact of adaptation on cell-fate heterogeneity and fractional killing. *Scientific Reports*, 10(1), 1–13.
- Matveeva, A., Fichtner, M., McAllister, K., McCann, C., Sturrock, M., Longley, D.B., and Prehn, J.H. (2019). Heterogeneous responses to low level death receptor activation are explained by random molecular assembly of

the caspase-8 activation platform. *PLoS computational biology*, 15(9), e1007374.

- Meyer, M., Paquet, A., Arguel, M.J., Peyre, L., Gomes-Pereira, L.C., Lebrigand, K., Mograbi, B., Brest, P., Waldmann, R., Barbry, P., et al. (2020). Profiling the non-genetic origins of cancer drug resistance with a single-cell functional genomics approach using predictive cell dynamics. *Cell systems*, 11(4), 367–374.
- Paek, A.L., Liu, J.C., Loewer, A., Forrester, W.C., and Lahav, G. (2016). Cell-to-cell variation in p53 dynamics leads to fractional killing. *Cell*, 165(3), 631–642.
- Péré, M., Chaves, M., and Roux, J. (2020). Core models of receptor reactions to evaluate basic pathway designs enabling heterogeneous commitments to apoptosis. In *International Conference on Computational Methods in Systems Biology*, 298–320. Springer.
- Purvis, J.E., Karhohs, K.W., Mock, C., Batchelor, E., Loewer, A., and Lahav, G. (2012). p53 dynamics control cell fate. *Science*, 336(6087), 1440–1444.
- Roux, J., Hafner, M., Bandara, S., Sims, J.J., Hudson, H., Chai, D., and Sorger, P.K. (2015). Fractional killing arises from cell-to-cell variability in overcoming a caspase activity threshold. *Molecular systems biology*, 11(5), 803.
- Strasser, A. and Vaux, D.L. (2020). Cell death in the origin and treatment of cancer. *Molecular Cell*.

Appendix A. DATA DESCRIPTION

Table A.1. Dataset description

TRAIL in ng/mL	T_0 in the model	# Total of cells	# Tolerant cells	# Sensitive cells
5	115	342	308	34
10	310	213	167	46
25	775	344	250	94
50	1550	414	114	300

Appendix B. AN IMPROVED FITTING METHOD

The improved fitting method follows 3 steps:

- (1) Estimate the FRETexp function (8) parameters with the *fit* function from the lmfit library.
- (2) Compute the corresponding reduced EAICR parameters using eq. (9).
- (3) Use the corresponding rEAICR parameters as initial guess for the method described in Péré et al. (2020).

Appendix C. CHARACTERISTIC TIME COMPUTATION

For sensitive cells, if τ_i is greater than the death time, $\tau_{i=}$ NaN; same for the resistant cells is $\tau_i > 24h$:

- i) $\tau_{T.trigger}$: $\arg\max_t Z_0(t)$, $t \in [0, 1]$
- ii) $\tau_{DISC.ass}$: $\min_t(t_1, t_2)$ with t_1 first time to satisfy $\dot{R}(t) < 5e-2$ (t_1 is the first time R stabilizes so its derivative gets close to 0), t_2 is the time when $pC8$ becomes linear with its coefficient equals to $-2\alpha_0 T_0$ so t_2 is the first time when $|pC8 + 2\alpha_0 T_0| < 5e-2$, and $5e-2$ being our threshold to consider the function closer enough to 0.
- iii) $\tau_{drug.0}$: $\arg\min_t T(t)$
- iv) $\tau_{DISC.end}$: t first time to satisfies $Z_0(t) > pC8(t)$
- v) $\tau_{C8.final}$: $\arg\min_t C8(t)$